



Delft University of Technology

Applications of Artificial Dielectric Layers for mm-Wave Antennas

Cavallo, Daniele

DOI

[10.1109/iWAT57058.2023.10171662](https://doi.org/10.1109/iWAT57058.2023.10171662)

Publication date

2023

Document Version

Final published version

Published in

2023 International Workshop on Antenna Technology, iWAT 2023

Citation (APA)

Cavallo, D. (2023). Applications of Artificial Dielectric Layers for mm-Wave Antennas. In *2023 International Workshop on Antenna Technology, iWAT 2023* (2023 International Workshop on Antenna Technology, iWAT 2023). IEEE. <https://doi.org/10.1109/iWAT57058.2023.10171662>

Important note

To cite this publication, please use the final published version (if applicable). Please check the document version above.

Copyright

Other than for strictly personal use, it is not permitted to download, forward or distribute the text or part of it, without the consent of the author(s) and/or copyright holder(s), unless the work is under an open content license such as Creative Commons.

Takedown policy

Please contact us and provide details if you believe this document breaches copyrights. We will remove access to the work immediately and investigate your claim.

Green Open Access added to TU Delft Institutional Repository

'You share, we take care!' - Taverne project

<https://www.openaccess.nl/en/you-share-we-take-care>

Otherwise as indicated in the copyright section: the publisher is the copyright holder of this work and the author uses the Dutch legislation to make this work public.

Applications of Artificial Dielectric Layers for mm-Wave Antennas

Daniele Cavallo
 Microelectronics dept.
 Delft University of Technology
 Delft, Netherlands
 ORCID: 0000-0003-1514-3656

Abstract—Artificial Dielectric Layers (ADLs) have recently been exploited to improve the radiation and impedance performance of integrated antennas at millimeter wave (mmWave) and terahertz (THz) frequencies. The ADLs are composed by layers of sub-wavelength periodic metal patches that can be arranged within a host medium to synthesize an equivalent anisotropic material. Thanks to the availability of closed-form expressions for the modeling, ADLs can be conveniently designed to realize matching layers and impedance transformers when used in the closed proximity of antennas, to improve their bandwidth and the front-to-back ratio. An overview of different applications that benefit from this concept is given. Moreover, recent developments on the use of ADLs for wideband flat lenses are described.

Keywords— artificial dielectrics, flat lenses, wideband arrays, wideband lenses

I. INTRODUCTION

Artificial dielectrics (ADs) were introduced in [1] as a light-weight alternative to real dielectric materials, for realizing microwave lenses [2]. After their introduction, ADs have been extensively studied and used for decades for radar development. An AD consists of a large-scale model of an actual dielectric, obtained by embedding conducting structures in a host material according to a regular pattern. Some physical realizations of ADs involve the insertion of metallic spheres, cylinder and strips inside a dielectric in a periodic arrangement. A specific type of AD, which is realized as a cascade of planar layers made of printed metal patches, is considered in this work and referred to as Artificial Dielectric Layers (ADLs), see Fig. 1(a). When such a structure is illuminated by an external electromagnetic field, the electric field scattered by the metal patches, when added to the incident field, creates an effective equivalent delay [3]. At the frequencies for which the periodicity of the pattern is much smaller than the wavelength, the structure can be assigned equivalent parameters that describe an anisotropic dielectric. The effective electric parameters can be engineered by varying the size of the metal obstacles and their spatial density. As shown in Fig. 1(b), the effective refractive index is function of the polarization of the wave, transverse electric (TE) or transverse magnetic (TM), and of the incidence angle θ . Such anisotropy is a key property of ADLs exploited in antenna design to avoid surface waves.

In this work, an overview of the application of ADLs for integrated high frequency antennas is given. Recently, ADLs have been employed as superstrates to improve the radiation performance of integrated antennas, both in the microwave [4] and the THz [5] frequency range. This approach is particularly beneficial for on-chip antennas, for which the maximum achievable efficiency is typically very low.

Planar designs of wideband arrays also can benefit from ADL slabs placed above the array to improve the matching performance and the scanning capability at mm-Wave

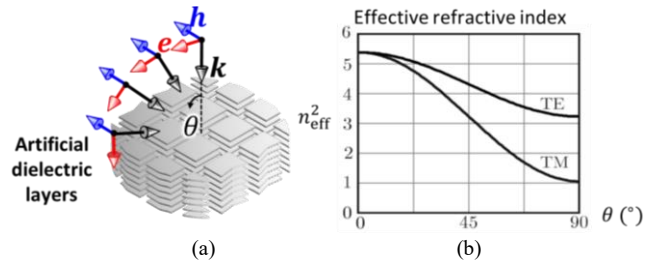


Fig. 1. (a) Artificial dielectric layers under plane wave incidence and (b) effective refractive index for transverse electric (TE) and transverse magnetic (TM) wave incidence, as a function of the incidence angle.

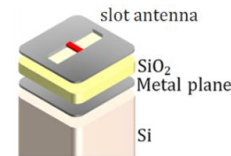


Fig. 2. Slot antenna on a silicon chip.

frequencies [6]. The artificial dielectrics can be used in combination with connected arrays [7] to achieve wide bandwidth over a large scan volume.

Moreover, the advance of mmWave technology for high-speed wireless communication and high-resolution radars has led to an increased popularity of dielectric lenses for multi-beam high-gain antennas [8]. It is shown that ADLs can also be used to design wideband flat lenses with low profile.

II. ADLS AS SUPERSTRATES

A. Limits of Integrated Antennas

On-chip antennas are characterized by poor radiation efficiency. A typical layer stack of a chip is shown in Fig. 2 and consists of a thin layer of silicon dioxide (SiO_2), about $10 \mu\text{m}$ thick, on which the antenna is realized (e.g., a slot antenna). A conducting metal plane separates the SiO_2 slab from a thick silicon (Si) layer. The metal plane has the purpose of shielding the antenna from the underlying silicon, since this latter is characterized by high losses. Because of the proximity of the antenna to the metal plane, in the case of slot radiators, most of the power remains confined within the SiO_2 layer, and thus is not radiated outside the chip (Fig. 3(a)). In some designs, the metal shield and the silicon are removed locally below the antenna. However, in this configuration, the antenna radiates equal power in the upper and lower half spaces, exhibiting a poor front-to-back ratio.

B. ADLs Superstrates for Efficient Integrated Antennas

A solution to mitigate these problems was proposed in [9]: by including an electrically dense material (superstrate) above the chip, the antenna tends to radiate predominantly in the direction of such material. This operation improves the performance of the device by improving the front-to-back

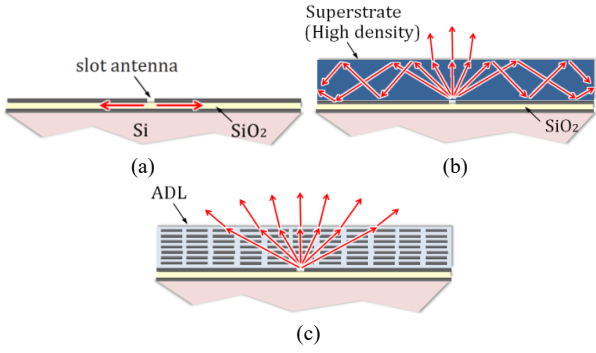


Fig. 3. (a) On-chip slot antenna close to a metal plane: power remains confined within the SiO₂ layer; (b) Standard superstrate: power couples into the dense material but is reflected at the material-air interface, generating surface waves; (c) ADL superstrate: power couples in the ADL material and is radiated outside the chip.

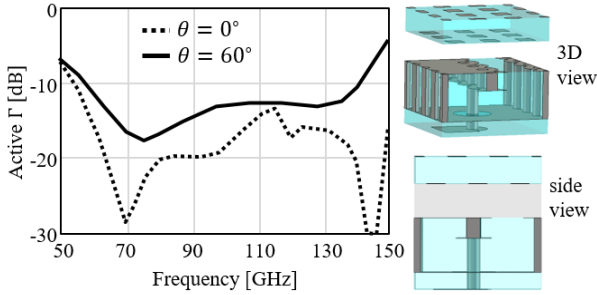


Fig. 4 Active reflection coefficient for broadside and scanning to 60 degrees in the E-plane for the unit cell in the inset.

ratio. However, the high density of the superstrate causes strong reflections at its top surface, resulting in a large portion of the power to be lost in surface waves, rather than being radiated. This is pictorially shown in Fig. 3(b).

In [5], ADLs were introduced as the solution to the surface-wave problem. Due to its anisotropy, the ADL synthesizes a slab with very high permittivity for rays that travel normal to the stratification, but low effective permittivity for angles tending to grazing (Fig. 1(b)). Thus total internal reflection at the interface between ADL and air hardly occurs, with very low power being launched into surface waves (see Fig. 3(c)). A 300 GHz on-chip-antenna with ADLs was manufactured and tested in [5], demonstrating the enhancement of the front-to-back ratio due to the ADLs.

C. ADLs Superstrates for Wideband Antenna Arrays

Another beneficial use of ADLs is in combination with planar wideband arrays, for example connected slot arrays [7]. One of the limits in wideband array design is the presence of the backing reflector, required to achieve unidirectional radiation. The presence of the backing reflector introduces a resonance, since the reflector has to be placed at about a quarter wavelength from the array plane. By enhancing the front-to-back ratio, ADLs reduce the amount of power radiated in the direction of the reflector, thus increasing the bandwidth of the array.

An example of array unit cell design was presented in [6] and shown in Fig. 4, which depicts a single-polarized connected slot element with ADL superstrate. The active reflection coefficient for broadside and for E-plane scanning to 60 degrees. This design has potential for application in dual-band automotive radar covering simultaneously the bands around 79 GHz and 140 GHz with 1-D scanning capabilities.

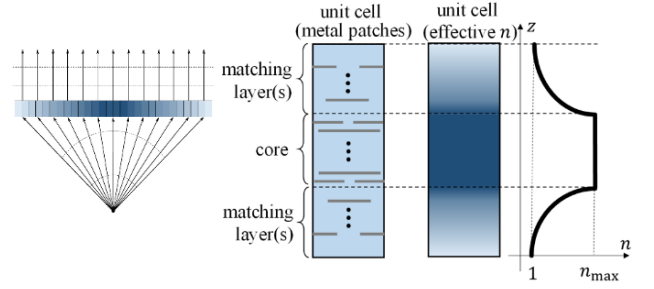


Fig. 5. Schematic of the gradient index lens and artificial dielectric unit cell to realize equivalent effective refractive index (n) gradient along z .

III. ARTIFICIAL DIELECTRIC LENSES

A. True Time Delay Lenses

Another application of ADLs is in the design of flat optics. Dielectric lenses are widely used in imaging and antenna systems, to provide high gain radiation characteristics and beam scanning or multi-beam capability. Conventional homogeneous dielectric lenses have excellent bandwidth and efficiency properties but are typically bulky and electrically thick. Thin flat lenses [10]-[12] are low profile and can be fabricated more easily compared to curved lenses, making them desirable at millimeter wave frequencies. Such low profile lenses are however band limited, because phase wrapping or resonant elements are used. To overcome the bandwidth limitations, one can employ true-time-delay (TTD) lenses that provide wideband behavior, at the cost of increased thickness. One possibility to reduce the thickness of wideband TTD lenses is to use high-permittivity materials [13]. To reduce the reflection losses that would be caused by the high permittivity, matching layers must be employed to improve the transmission at the air-lens interface [14]. ADLs [15] can be used to realize TTD flat lens, by achieving high refractive indexes for the core of the lens and low reflection through matching layers.

To design a flat lens that converts a spherical wavefront into a planar one, the lens has to provide a phase shift that is larger in the center and smaller towards the lens edges (Fig. 5). The lens is divided in unit cells, each consisting of a dense core layer to provide the required phase shift and two matching layer sections to reduce reflections. All sections can be synthesized by ADLs as shown in Fig. 5, using the closed-form analysis reported in [16].

B. Example of Lens Design

This section details a design example of a flat lens based on ADLs in printed circuit board (PCB) technology, operating over an octave bandwidth. The operating frequency band is 70-140 GHz. The lens diameter is $11.6 \lambda_0$, where λ_0 is the free-space wavelength at the maximum frequency. This corresponds to a maximum directivity of 31dB. The focal ratio $F/D = 1$. The above requirements result in a maximum phase variation of 477° . The dielectric material for the lens is chosen as Rogers RO4350B, with the following properties and constraints:

- Minimum gap width between patches in PCB is 80 μ m.
- Relative permittivity of hosting medium $\epsilon_r = 3.66$.
- Minimum distance between patch layers is 100 μ m.

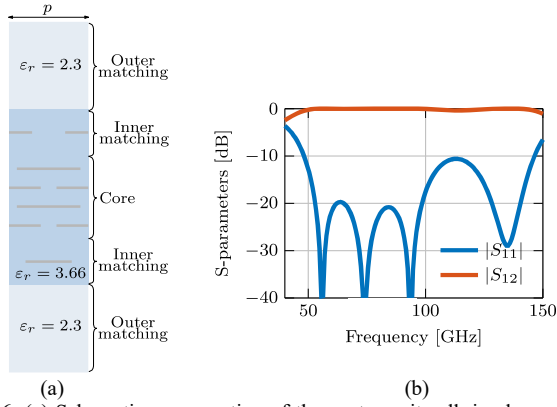


Fig. 6. (a) Schematic cross section of the center unit cell, implemented as ADLs; (b) correspondent reflection coefficient S_{11} and transmission coefficient S_{12} .

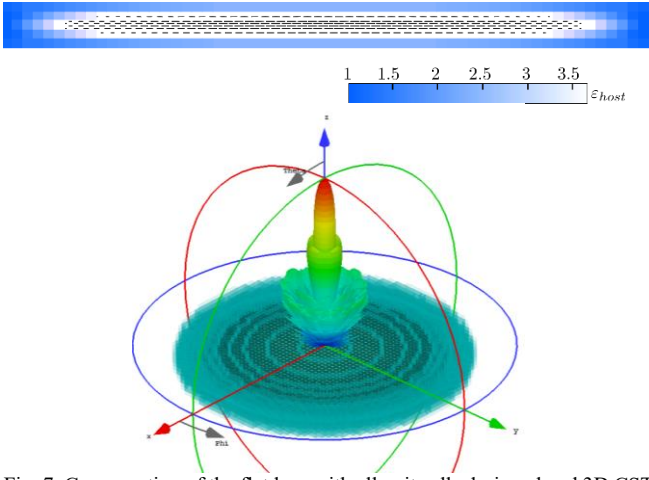


Fig. 7. Cross-section of the flat lens with all unit cells designed and 3D CST model of the lens.

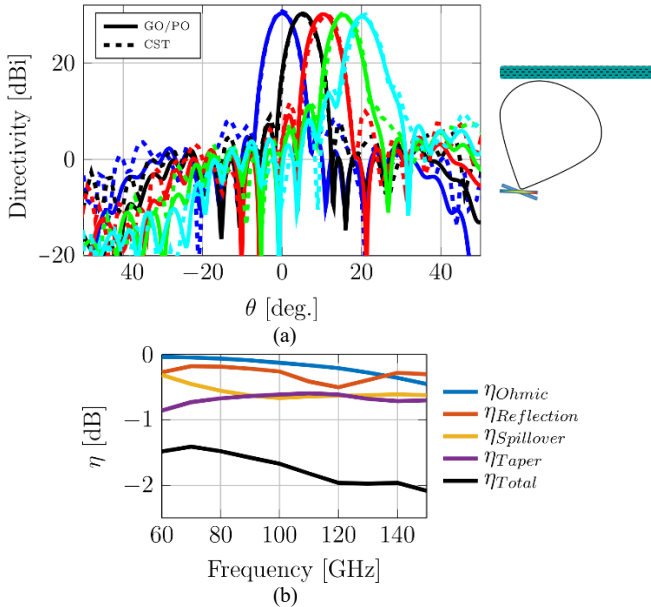


Fig. 8. (a) Directivity at 140 GHz of the example flat lens design, for different lateral displacements of the feed. (b) Efficiencies for the broadside beam.

Besides the material-related constraints, the period of the ADL is chosen as $0.19 \lambda_0$, to keep the size of the patches sub-wavelength. The maximum effective permittivity, using the given material properties and manufacturing constraints, is

$\epsilon_{r,\max} = 19$. With a 2-section Chebyshev transformer, a core thickness of 0.41mm is sufficient to achieve the required total phase variation of 477° in the center of the lens. The total unit cell thickness is 1.8mm , or $0.85\lambda_0$.

Considering the constraints defined before, one can synthesize the center unit cell. The realized center unit cell is shown in Fig. 6, and achieves reflection coefficient $< -10\text{dB}$ over the entire bandwidth of operation. The core and inner layer are implemented using ADLs, the outer matching layer as a homogeneous dielectric. The unit cell has 6 metal layers in total. All other unit cells are derived from the center unit cell, altering the geometrical parameters of ADLs in the core and matching layers to provide the required phase shift. A cross-section of the final lens design is shown in Fig. 7.

To assess the performance of the lens, a combined geometrical optics (GO) / physical optics (PO) approach is used to evaluate the radiation patterns and efficiency. Each GO ray is studied as a plane wave problem to find the S -parameters of the unit cell it impinges on, under local periodicity assumption.

The feed is assumed to be a planar current distribution in the focal plane. If the feed is displaced laterally, the main beam of the feed is assumed to be repointed to the center of the lens by applying a tilt of a linear phase shift, to improve the spillover efficiency, as shown in the inset of Fig. 8(a).

Using the radiated field from the feed, plane waves impinging on each of the unit cells are computed. To find the transmitted electric field after the lens, the $\hat{\theta}$ - and $\hat{\phi}$ -components of the incident electric field before the lens are multiplied by the S_{12} of the unit cell for the TM- and TE-modes, respectively. Local periodicity is assumed when computing the S -parameters of each unit cell. From the electric field after the lens, by applying the equivalence theorem, the equivalent PO surface currents after the lens can be used to compute the far-field radiation pattern.

In Fig. 8(a) the far-field radiation patterns of the flat lens illuminated at 140 GHz are shown. The feed is assumed to be an ideal Gaussian feed illuminating the lens with -10dB edge taper at all frequency under investigation. The estimate of the maximum directivity, as well as the shape of the main beam, computed using the GO/PO method is close to the results from the CST simulations. It is worth noting that the computation time for the GO/PO approach is only a few seconds to compute each pattern, while it is in the order of a few hours for CST.

The efficiencies of the presented design example are presented for the broadside beam in Fig. 8(b), highlighting the wideband and highly efficient characteristics of the proposed ADL lens concept. A number of other examples of lens designs for mmWave applications will be shown at the conference.

IV. CONCLUSION

The use of artificial dielectric layers for the design of high-efficiency mmWave and THz antennas was discussed. ADLs increase the front-to-back ratio of antennas radiating in their proximity, thus mitigating the negative effect of the ground plane located below the antenna. Thanks to the anisotropy, ADLs do not support surface waves like standard homogenous dielectric. ADLs are also suitable to design

wideband flat lenses with true-time-delay properties. An example design operating from 70 to 140 GHz was presented.

REFERENCES

- [1] W. E. Kock, "Metallic delay lenses," *Bell System Tech. J.*, vol. 27, no. 1, pp. 58-82, Jan. 1948.
- [2] S. S. D. Jones and J. Brown, "Metallic delay lenses," *Nature*, vol. 163, no. 4139, pp. 324-325, Feb. 1949.
- [3] R. E. Collin, *Field Theory of Guided Waves, 2nd Ed.*, IEEE Press, New York, 1991.
- [4] W. H. Syed and A. Neto, "Front-to-back ratio enhancement of planar printed antennas by means of artificial dielectric layers," *IEEE Trans. Antennas Propag.*, vol. 61, no. 11, pp. 5408-5416, Nov. 2013.
- [5] W. H. Syed, G. Fiorentino, D. Cavallo, M. Spirito, P. M. Sarro, and A. Neto, "Design, fabrication and measurement of 0.3 THz on-chip double-slot antenna enhanced by artificial dielectrics," *IEEE Trans. THz Sci. Tech.*, vol. 5, no. 2, pp. 288-298, Mar. 2015.
- [6] D. Cavallo, "Parallel-plate waveguide-feeding structure for planar-connected arrays," *IEEE Antennas Wirel. Propag. Lett.*, vol. 21, no. 4, pp. 765-768, Apr. 2022
- [7] W. H. Syed, D. Cavallo, H. T. Shivamurthy, and A. Neto, "Wideband, wide-scan planar array of connected slots loaded with artificial dielectric superstrates," *IEEE Trans. Antennas Propag.*, vol. 64, no. 2, pp. 543-553, Feb. 2016.
- [8] W. Hong et al., "Multibeam antenna technologies for 5G wireless communications," *IEEE Trans. Antennas Propag.*, vol. 65, no. 12, pp. 6231-6249, Dec. 2017.
- [9] J. M. Edwards and G. M. Rebeiz, "High-efficiency elliptical slot antennas with quartz superstrates for silicon RFICs," *IEEE Trans. Antennas Propag.*, vol. 60, no. 11, pp. 5010-5020, Nov. 2012.
- [10] A. Jouade, M. Himdi, and O. Lafond, "Fresnel lens at millimeter-wave: enhancement of efficiency and radiation frequency bandwidth," *IEEE Trans. Antennas Propag.*, vol. 65, no. 11, pp. 5776-5786, Nov. 2017.
- [11] G. Liu, M. R. Dehghani Kodnoeih, K. T. Pham, E. M. Cruz, D. González-Ovejero, and R. Sauleau, "A millimeter-wave multibeam transparent transmitarray antenna at Ka-Band," *IEEE Antennas Wireless Propag. Lett.*, vol. 18, no. 4, pp. 631-635, Apr. 2019.
- [12] M. Jiang, Z. N. Chen, Y. Zhang, W. Hong, and X. Xuan, "Metamaterial-based thin planar lens antenna for spatial beamforming and multibeam massive MIMO," *IEEE Trans. Antennas Propag.*, vol. 65, no. 2, pp. 464-472, Feb. 2017.
- [13] F. Maggiorelli, A. Paraskevopoulos, J. C. Vardaxoglou, M. Albani, and S. Maci, "Profile inversion and closed form formulation of compact GRIN lenses," *IEEE Open J. Antennas Propag.*, vol. 2, pp. 315-325, 2021.
- [14] N. C. Garcia and J. D. Chisum, "High-efficiency, wideband GRIN lenses with intrinsically matched unit cells," *IEEE Trans. Antennas Propag.*, vol. 68, no. 8, pp. 5965-5977, Aug. 2020.
- [15] M. Li and N. Behdad, "Wideband true-time-delay microwave lenses based on metallo-dielectric and all-dielectric lowpass frequency selective surfaces," *IEEE Trans. Antennas Propag.*, vol. 61, no. 8, pp. 4109-4119, Aug. 2013.
- [16] D. Cavallo and R. M. van Schelven, "Closed-form analysis of artificial dielectric layers with non-periodic characteristics," *Proc. Eur. Conf. Antennas Propag.*, Krakow, Poland, 31 Mar.-5 Apr. 2019, pp. 1-5.